CARBON letters

Note

Carbon Letters Vol. 20, 66-71 (2016)

Effect of acid catalysts on carbonization temperatures for ordered mesoporous carbon materials

Jeong Kuk Shon, Xing Jin, Yun Seok Choi, Jong Gu Won, Yoon Kyung Hwang, Dae Jong You, Chengbin Li and Ji Man Kim*

Department of Chemistry, Sungkyunkwan University, Suwon 16419, Korea

Article Info

Received 11 January 2016
Accepted 9 May 2016

***Corresponding Author**
E-mail: jimankim@skku.edu
Tel: +82-31-290-5930

Open Access

DOI: http://dx.doi.org/10.5714/CL.2016.20.066

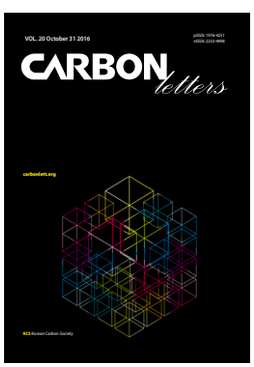

http://carbonlett.org

pISSN: 1976-4251
eISSN: 2233-4998

Highly ordered mesoporous carbon (OMC) materials have attracted much attention in many fields including catalysis, adsorption and energy storage, due to their high porosity, high surface area and controllable regular pore-structure [1-6]. Successful synthesis pathways for obtaining OMC materials include the direct synthesis of OMC materials through the organic-organic self-assembly method (soft templating process) and nano-replication of OMC materials from mesoporous silica templates (hard templating process) [7-11]. The direct synthesis method is suitable for large-scale production of carbon materials due to its easier process compared to the nano-replication method [7,8]. However, the nano-replication method has still several advantages for synthesizing OMC materials. It is possible to synthesize various kinds of mesostructured OMC materials, which can be controlled by the mesostructure of the silica templates [12,13]. In addition, the morphology of OMC materials can also be varied with the silica templates using desired morphologies [12-14]. More importantly, various kinds of carbon precursors including sucrose, furfural, *p*-toluene sulfonic acid (*p*-TSA) and phenanthrene [14-17] can be used to control the physicochemical properties of the OMC materials, for which the nature of the carbon precursors affects the conductivity, porosity and surface functionality of the carbon frameworks [17-19]. However, nano-replication methods for OMC materials, based on a conventional thermal process at high temperature (typically above 900°C), are time- and energy-consuming processes. In order to oligomerize or polymerize the carbon precursors before the carbonization, an aging process should also be carried out in the presence of acid catalysts in low temperature ranges of 100°C–200°C. In the case of sucrose as a carbon source, sulfuric acid (H_2SO_4) is typically used as an acid catalyst for the dehydration and subsequent oligomerization of the carbon precursor. This is very important for preventing the infiltrated carbon precursors from draining outside the mesopores of the silica templates before the carbonization. The oligomeric carbon species are then carbonized at high temperature above 600°C.

Despite using sulfuric acid which has a good carbonization ability as a carbonization catalyst, OMC with a well-developed mesostructure is not obtained at carbonization temperatures below 600°C [20]. Low carbonization temperatures (<600°C) for the synthesis of OMC materials are very important for achieving process economics and, in particular, for enhancing diversity. For various applications of OMC materials, it is necessary that heteroatom species, such as nitrogen and sulfur, are included in a final OMC product from the initial precursor mixture for the synthesis of OMC. However, carbonization temperatures above 600°C are too high to maintain the functionality of heteroatoms; thus, to achieve this aim, a low-temperature carbonization process should be addressed in the future.

In the present work, we investigated the effect of acid catalysts in connection with the carbonization temperature for the synthesis of OMC materials. *p*-toluene sulfonic acid (*p*-TSA, $CH_3C_6H_4SO_3H$), phosphoric acid (H_3PO_4), sulfuric acid (H_2SO_4), nitric acid (HNO_3), hydrochloric acid (HCl), and acetic acid (CH_3COOH) were used as the acid catalysts for carbonization. As a result, unlike other acid catalysts, the use of *p*-TSA and phosphoric acid produces OMC materials with a well-developed mesostructure at low carbonization tem-

peratures ranging from 300°C to 500°C.

The synthesis of the OMC was done with a general nanoreplication method. A mesoporous silica KIT-6 with a 3-d cubic mesostructure (Fig. S1) and sucrose were used as the silica template and the carbon precursor, respectively [21,22]. For oligomerization and dehydration, various kinds of acid catalysts including *p*-TSA, H_3PO_4, H_2SO_4, HNO_3, HCl, and acetic acid were used. After infiltration of the carbon precursor and the acid catalyst within the mesopores of the KIT-6 template, the carbon materials were obtained by carbonization at temperatures ranging from 300°C to 900°C for 2 h under a N_2 atmosphere. The OMC materials thus obtained are denoted as OMC-*x*-*T*, where *x* means the acid catalyst used (i.e., *x* = TSA [*p*-toluene sulfonic acid], P [phosphoric acid], S [sulfuric acid], N [nitric acid], H [hydrochloric acid], A [acetic acid], and No [no acid catalyst]) and *T* indicates the corresponding carbonization temperature. After carbonization, the mesoporous silica template was removed with an aqueous solution of hydrofluoric acid (HF, 20 wt%).

X-ray diffraction (XRD) patterns of the OMC materials were obtained in the reflection mode with a Rigaku D/MAX-2200 Ultima equipped with Cu K_α radiation at 30 kV and 40 mA. Transmission electron microscopy (TEM) images were obtained with a JEOL JEM 3010 at an accelerating voltage of 300 kV. N_2 adsorption–desorption isotherms were collected with a Micromeritics Tristar system at the liquid N_2 temperature. All of the samples were completely dried under vacuum at 120°C for 24 h before the measurements. Specific Brunauer-Emmett-Teller surface areas were calculated from the adsorption branches in a relative pressure range (p/p_0) from 0.05 to 0.20. Pore-size distribution curves were obtained from the adsorption branches by the Barrett-Joyner-Halenda (BJH) method. The real density of all the OMC-*x*-*T* materials was analyzed with a Micromeritics Gas Pycnometer system using helium gas. All of the samples were also dried under vacuum at 120°C for 24 h before the measurements. The real density value of each OMC-*x*-*T* material was estimated from an average of more than 60 measurements, respectively.

Fig. 1 shows the small-angle XRD patterns of the OMC-*x*-*T* materials. The mesostructure of the prepared OMC materials at 900°C, which is the typical carbonization temperature, shows XRD patterns corresponding to the typical *Ia*3*d* ([211] and [220] peaks) by the long-range ordering of the OMC samples, except for the OMC-A-900 and OMC-No-900 materials. However, the XRD patterns from the OMC-*x*-600 and OMC-*x*-300 materials changed significantly depending on the acid catalysts. As shown in Fig. 1 and Fig. S2, the intensity of the XRD peaks gradually decreases as the carbonization temperature decreases. Most of the OMC-*x*-300 materials do not form a good mesostructured carbon framework. Nevertheless, the OMC-TSA-300 and OMC-P-300 materials had specific XRD patterns corresponding to mesostructured carbon frameworks. As seen in Fig. S2, the OMC-TSA-*T* materials, obtained through carbonization under 500°C, exhibit a new peak that corresponds to the position of the (110) reflection peak, and all of the OMC-S-*T* materials show the corresponding (110) reflection peak. However, the (110) reflection peak is not observed in the case of the OMC-P-*T* materials, regardless of the temperature range for carbonization. The presence of a (110) reflection is known to be a phase transition from the cubic *Ia*3*d* symmetry to the tetragonal $I4_{1/a}$ (or lower) symmetry after the removal of the silica template [16,23]. The OMC materials with a well-developed *Ia*3*d* mesostructure is maintained by interconnecting thin pillars, which are formed inside the micropores connecting two different mesopores of the KIT-6 templates. The rigidity of interconnecting pillars seems to be related to the degree of carbonization. Based on this, the observance of a (110) reflection peak can be used as a relative indicator for the degree of carbonization. Thus, the data suggest that phosphoric acid exhibits the best carbonization ability at lower temperatures among the acid catalysts used in the present work.

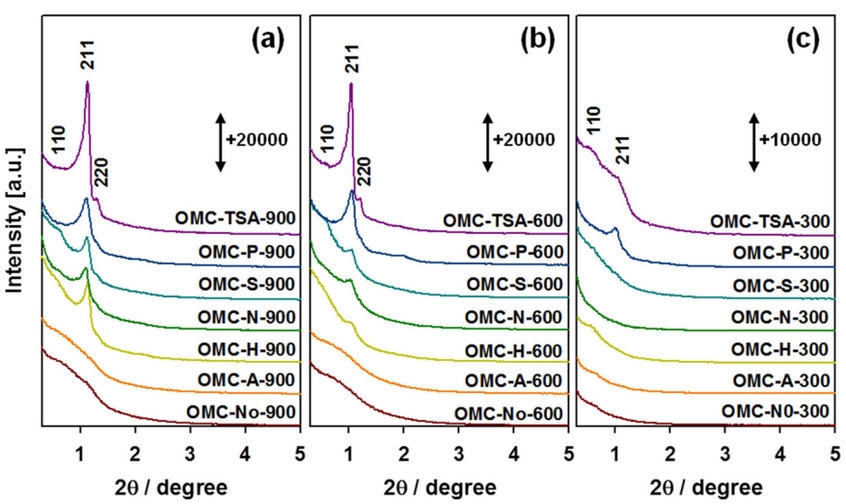

Fig. 1. Small-angle X-ray diffraction patterns of the (a) OMC-*x*-900, (b) OMC-*x*-600, and (c) OMC-*x*-300 materials obtained with different acid catalysts. OMC, ordered mesoporous carbon; TSA, *p*-toluene sulfonic acid; P, phosphoric acid; S, sulfuric acid; N, nitric acid; H, hydrochloric acid; A, acetic acid; No, no acid catalyst.

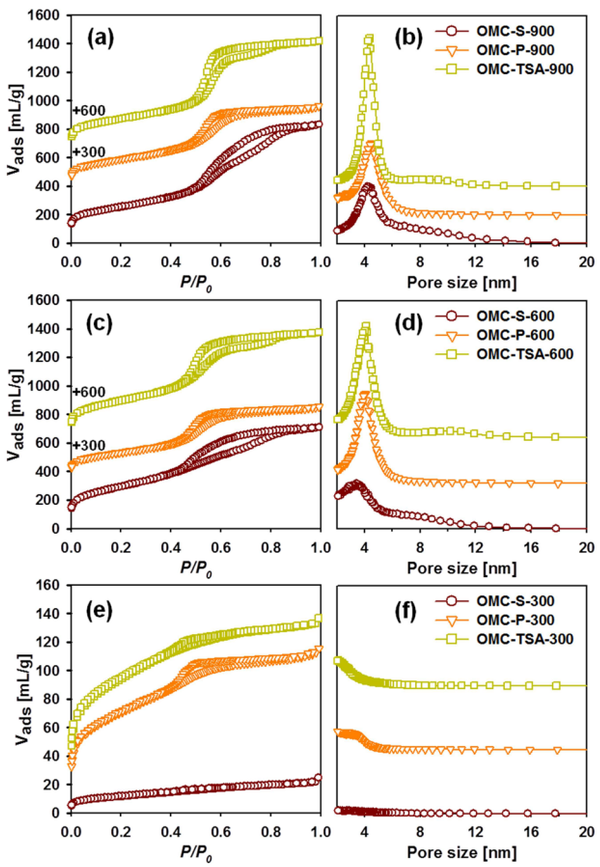

Fig. 2. N_2 adsorption-desorption isotherms and the corresponding Barrett-Joyner-Halenda pore size distribution curves of the OMC-TSA-*T*, OMC-P-*T* and OMC-S-*T* materials: (a, b) 900°C, (c, d) 600°C, and (e, f) 300°C. OMC, ordered mesoporous carbon; TSA, *p*-toluene sulfonic acid; P, phosphoric acid; S, sulfuric acid.

Fig. 2 shows the N_2 adsorption-desorption isotherms and the corresponding BJH pore-size distribution curves for the OMC-TSA-*T*, OMC-P-*T* and OMC-S-*T* materials obtained at different carbonization temperatures. The physical properties calculated from the XRD and N_2 adsorption-desorption data for the OMC-TSA-*T*, OMC-P-*T* and OMC-S-*T* materials are summarized in Table 1. The N_2 adsorption-desorption data exhibit tendencies similar to the XRD patterns. The isotherm curve of OMC-S-300 showed a very low N_2 adsorption amount and no capillary condensation while the OMC-S-600 and OMC-S-900 showed typical type-IV isotherms with hysteresis loops. Moreover, the OMC-TSA-300 and OMC-P-300 materials had type-IV isotherms with hysteresis loops from the formation of mesopores even at a low carbonization temperature of 300°C. Thus, the *p*-TSA and phosphoric acid are very effective as acid catalysts for OMC synthesis under a carbonization process at low temperatures. Surface areas and total pore volumes of the OMC-*x*-300 materials show remarkable differences depending on the type of acid catalyst used (Table 1). The excellent carbonization abilities of the *p*-TSA and phosphoric acid was also confirmed by the N_2 adsorption-desorption analysis among the OMC-*x*-300 materials (Table S1 and Fig. S3).

Table 1. Physicochemical properties of the OMC-TSA-*T*, OMC-P-*T* and OMC-S-*T*

Material	$a^{a)}$ (nm)	$S_{BET}{}^{b)}$ (m^2/g)	$V_{tot}{}^{c)}$ (cc/g)	$D_{BJH}{}^{d)}$ (nm)
OMC-TSA-900	19.1	977	1.27	4.3
OMC-P-900	19.4	1035	1.02	4.5
OMC-S-900	19.3	903	1.29	4.1
OMC-TSA-600	20.9	1076	1.20	4.1
OMC-P-600	20.5	832	0.86	4.1
OMC-S-600	20.5	1055	1.10	3.6
OMC-TSA-300	22.0	340	0.21	-
OMC-P-300	21.6	255	0.18	3.3
OMC-S-300	-	41	0.04	-

OMC, ordered mesoporous carbon; TSA, *p*-toluene sulfonic acid; P, phosphoric acid; S, sulfuric acid.
[a)]Lattice parameters calculated from the (211) X-ray diffraction peaks of the materials.
[b)]Brunauer-Emmett-Teller surface areas calculated in the relative pressure (p/p_0) range from 0.05 to 0.20.
[c)]Total pore volume measured at a p/p_0 of 0.99.
[d)]Barrett-Joyner-Halenda pore sizes obtained from the adsorption branches.

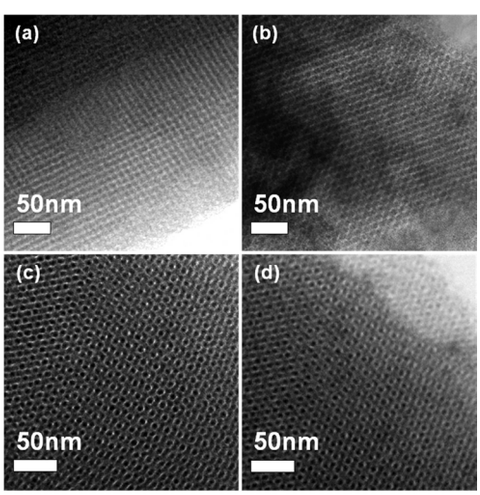

Fig. 3. Transmission electron microscopy images of the (a) OMC-TSA-300, (b) OMC-P-300, (c) OMC-TSA-900, and (d) OMC-P-900 materials. OMC, ordered mesoporous carbon; TSA, *p*-toluene sulfonic acid; P, phosphoric acid.

Fig. 3 shows the TEM images of the typical OMC-TSA-*T* and OMC-P-*T* materials obtained by carbonization at 300°C and 900°C, respectively. The OMC-TSA-900 and OMC-P-900 materials (Fig. 3c and d) clearly show a well-developed and well-aligned cubic mesostructure. The TEM images show that the carbonized OMC-TSA-300 and OMC-P-300 materials also have a comparatively good mesostructure. To

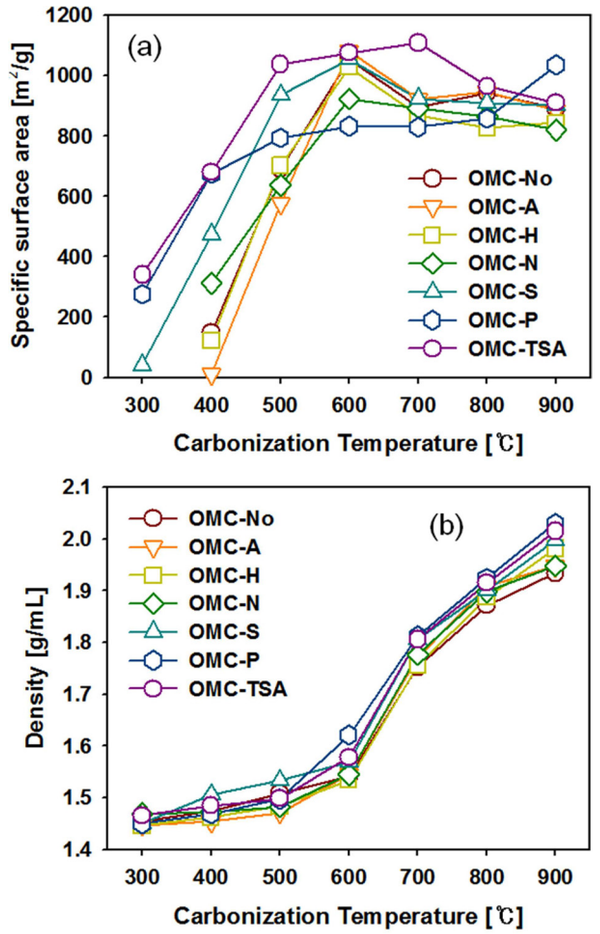

Fig. 4. Plots of (a) specific surface areas and (b) real densities of the OMC-*x*-*T* materials obtained at carbonization temperatures ranging from 300°C to 900°C. OMC, ordered mesoporous carbon; No, no acid catalyst; A, acetic acid; H, hydrochloric acid; N, nitric acid; S, sulfuric acid; P, phosphoric acid; TSA, *p*-toluene sulfonic acid.

elucidate the reason for the excellent carbonization ability of *p*-TSA and phosphoric acid, the specific surface areas and real densities of all the OMC materials are plotted against the carbonization temperatures in Fig. 4. According to these data, the carbonization process for preparing OMC materials might be divided into two regions: a low-carbonization temperature region (<600°C) and a high-carbonization temperature region (>600°C). Fig. 4 shows that the surface areas of all the OMC materials increase as the carbonization temperature increases up to 600°C and are saturated above 600°C, whereas the real densities are very similar below 600°C (~1.5 g/mL), and there is a rapid increase after this temperature which is probably due to the remarkable contraction of the carbon framework and the removal of other species except for the carbon element at high temperatures. The carbonization might mainly be attributed only to the heat (thermal carbonization) in the high-carbonization temperature region, where the acid catalysts do not exist due to their decomposition or gasification. In contrast, in the carbonization processes in the low-carbonization temperature region, carbonization is progressed by both the acid catalyst (catalytic carbonization) and the heat simultaneously. The more the carbonization temperature decreases, the more the catalytic carbonization from the catalytic carbonization process prevails over the thermal carbonization. Consequently, for the synthesis of OMC materials at low temperatures, the carbonization ability of the acid catalyst is the most important factor.

To further understand the relationship between the carbonization ability and the acidity, the pK_a values for each acid catalyst are listed in Table S2. The pK_a tendency of the acid catalysts does not correspond with the degree of mesostructure development of the OMC materials in the low-carbonization temperature region (<600°C). The XRD and N_2 sorption data (Figs. S2 and S3 and Table S1) indicate that both the strong acids (HCl, HNO_3, and H_2SO_4) and the weak acid (CH_3COOH) do not result in the formation of ordered mesostructures below 600°C, whereas the use of *p*-TSA and phosphoric acid with relatively moderate acid strengths yields high-quality OMC materials at low temperatures. The acidity strength, based on the pK_a value, is not a factor of the carbonization ability at low temperatures. Thus, the stability of the acid catalysts during carbonization is the reason for the low temperature carbonization. The carbonization ability of acid catalysts for OMC materials at a low temperature depends on the degree of surviving acid catalyst during carbonization. The retention of the acid catalyst within the pores of the silica template is important at low temperatures (<600°C) for the polymerization and dehydration of the carbon precursor. In this manner, the features of *p*-TSA, phosphoric acid, and sulfuric acid can be described as follows. *p*-TSA, phosphoric acid, and sulfuric acid have relatively higher boiling points than that of the other acid catalysts (Table S2), which means that these acid catalysts can help carbonization more continuously in the low-carbonization temperature region than that of the other acid catalysts. Moreover, the *p*-TSA catalyst can have the role of a carbon precursor as well as an acid catalyst because the OMC material can be obtained with only *p*-TSA without any other carbon precursors [24]. In the case of the phosphoric acid, its excellent carbonization ability is mainly due to the formation of polymer-type phosphoric acids, such as pyrophosphoric acid and metaphosphoric acid, with increasing temperature [25-27]. In particular, phosphoric acid has a high carbonization ability at low temperatures which is due to such phase transformations.

In this study, various kinds of acids as carbonization catalysts were used for the synthesis of ordered mesoporous carbon materials. It was found that *p*-toluene sulfuric acid and phosphoric acid were very effective carbonization catalysts at low temperatures compared with the other acid catalysts including sulfuric acid, hydrochloric acid, nitric acid and acetic acid. These results may be attributed to the stability of the acid catalysts during the carbonization rather than the acidity strength. *p*-toluene sulfuric acid and phosphoric acid yield ordered mesoporous carbon materials by the double role as a carbon precursor and an acid catalyst for carbonization and by transforming into a polymer-type acid at low temperatures (<600°C), respectively.

Conflict of Interest

No potential conflict of interest relevant to this article was reported.

Acknowledgements

This work was supported by the Energy Efficiency and Resources Core Technology program (No. 20132020000260) of the Korea Institute of Energy Technology Evaluation and Planning (KETEP) with financial resources from the Ministry of Trade, Industry and Energy. We also would like to thank the partial support from the Degree and Research Center (DRC) program (2014) through the National Research Council of Science & Technology (NST) from the Ministry of Science, ICT and Future Planning.

References

[1] Joo SH, Choi SJ, Oh I, Kwak J, Liu Z, Terasaki O, Ryoo R. Ordered nanoporous arrays of carbon supporting high dispersions of platinum nanoparticles. Nature, **412**, 169 (2001). http://dx.doi.org/10.1038/35084046.

[2] Su F, Lee FY, Lv L, Liu J, Tian XN, Zhao XS. Sandwiched ruthenium/carbon nanostructures for highly active heterogeneous hydrogenation. Adv Funct Mater, **17**, 1926 (2007). http://dx.doi.org/10.1002/adfm.200700067.

[3] Hartmann M, Vinu A, Chandrasekar G. Adsorption of vitamin E on mesoporous carbon molecular sieves. Chem Mater, **17**, 829 (2005). http://dx.doi.org/10.1021/cm048564f.

[4] Joo SH, Kwon K, You DJ, Pak C, Chang H, Kim JM. Preparation of high loading Pt nanoparticles on ordered mesoporous carbon with a controlled Pt size and its effects on oxygen reduction and methanol oxidation reactions. Electrochim Acta, **54**, 5746 (2009). http://dx.doi.org/10.1016/j.electacta.2009.05.022.

[5] Saha D, Deng S. Enhanced hydrogen adsorption in ordered mesoporous carbon through clathrate formation. Int J Hydrogen Energy, **34**, 8583 (2009). http://dx.doi.org/10.1016/j.ijhydene.2009.08.047.

[6] Xia Y, Walker GS, Grant DM, Mokaya R. Hydrogen storage in high surface area carbons: experimental demonstration of the effects of nitrogen doping. J Am Chem Soc, **131**, 16493 (2009). http://dx.doi.org/10.1021/ja9054838.

[7] Meng Y, Gu D, Zhang F, Shi Y, Yang H, Li Z, Yu C, Tu B, Zhao D. Ordered mesoporous polymers and homologous carbon frameworks: amphiphilic surfactant templating and direct transformation. Angew Chem, **43**, 7215 (2005). http://dx.doi.org/10.1002/ange.200501561.

[8] Tanaka S, Nishiyama N, Egashira Y, Ueyama K. Synthesis of ordered mesoporous carbons with channel structure from an organic-organic nanocomposite. Chem Commun, (16), 2125 (2005). http://dx.doi.org/10.1039/B501259G.

[9] Ryoo R, Joo SH, Jun S. Synthesis of highly ordered carbon molecular sieves via template-mediated structural transformation. J Phys Chem B, **103**, 7743 (1999). http://dx.doi.org/10.1021/jp991673a.

[10] Ryoo R, Joo SH, Kruk M, Jaroniec M. Ordered mesoporous carbons. Adv Mater, **13**, 677 (2001). http://dx.doi.org/10.1002/1521-4095(200105)13:9<677::AID-ADMA677>3.0.CO;2-C.

[11] Lee HI, Stucky GD, Kim JH, Pak C, Chang H, Kim JM. Spontaneous phase separation mediated synthesis of 3D mesoporous carbon with controllable cage and window size. Adv Mater, **23**, 2357 (2011). http://dx.doi.org/10.1002/adma.201003599.

[12] Yang H, Zhao D. Synthesis of replica mesostructures by the nanocasting strategy. J Mater Chem, **15**, 1217 (2005). http://dx.doi.org/10.1039/B414402C.

[13] Lu AH, Schüth F. Nanocasting: a versatile strategy for creating nanostructured porous materials. Adv Mater, **18**, 1793 (2006). http://dx.doi.org/10.1002/adma.200600148.

[14] Joo SH, Lee HI, You DJ, Kwon K, Kim JH, Choi YS, Kang M, Kim JM, Pak C, Chang H, Seung D. Ordered mesoporous carbons with controlled particle sizes as catalyst supports for direct methanol fuel cell cathodes. Carbon, **46**, 2034 (2008). http://dx.doi.org/10.1016/j.carbon.2008.08.015.

[15] Kruk M, Jaroniec M, Kim TW, Ryoo R. Synthesis and characterization of hexagonally ordered carbon nanopipes. Chem Mater, **15**, 2815 (2003). http://dx.doi.org/10.1021/cm034087+.

[16] Kim TW, Solovyov LA. Synthesis and characterization of large-pore ordered mesoporous carbons using gyroidal silica template. J Mater Chem, **16**, 1445 (2006). http://dx.doi.org/10.1039/B516945C.

[17] Joo SH, Pak C, You DJ, Lee SA, Lee HI, Kim JM, Chang H, Seung D. Ordered mesoporous carbons (OMC) as supports of electrocatalysts for direct methanol fuel cells (DMFC): effect of carbon precursors of OMC on DMFC performances. Electrochim Acta, **52**, 1618 (2006). http://dx.doi.org/10.1016/j.electacta.2006.03.092.

[18] Darmstadt H, Roy C, Kaliaguine S, Kim TW, Ryoo R. Surface and pore structures of CMK-5 ordered mesoporous carbons by adsorption and surface spectroscopy. Chem Mater, **15**, 3300 (2003). http://dx.doi.org/10.1021/cm020673b.

[19] Fuertes AB, Centeno TA. Mesoporous carbons with graphitic structures fabricated by using porous silica materials as templates and iron-impregnated polypyrrole as precursor. J Mater Chem, **15**, 1079 (2005). http://dx.doi.org/10.1039/B416007J.

[20] Lee HI, Kim JH, Joo SH, Chang H, Seung D, Joo OS, Suh DJ, Ahn WS, Pak C, Kim JM. Ultrafast production of ordered mesoporous carbons via microwave irradiation. Carbon, **45**, 2851 (2007). http://dx.doi.org/10.1016/j.carbon.2007.08.031.

[21] Kleitz F, Choi SH, Ryoo R. Cubic Ia3d large mesoporous silica: synthesis and replication to platinum nanowires, carbon nanorods and carbon nanotubes. Chem Commun, (17), 2136 (2003). http://dx.doi.org/10.1039/B306504A.

[22] Kim TW, Kleitz F, Paul B, Ryoo R. MCM-48-like large mesoporous silicas with tailored pore structure: facile synthesis domain in a ternary triblock copolymer-butanol-water system. J Am Chem Soc, **127**, 7601 (2005). http://dx.doi.org/10.1021/ja042601m.

[23] Solovyov LA, Zaikovskii VI, Shmakov AN, Belousov OV, Ryoo R. Framework characterization of mesostructured carbon CMK-1 by X-ray powder diffraction and electron microscopy. J Phys Chem B, **106**, 12198 (2002). http://dx.doi.org/10.1021/jp0257653.

[24] Lee HI, Joo SH, Kim JH, You DJ, Kim JM, Park JN, Chang H, Pak C. Ultrastable Pt nanoparticles supported on sulfur-containing ordered mesoporous carbon via strong metal-support interaction. J Mater Chem, **19**, 5934 (2009). http://dx.doi.org/10.1039/B907514C.

[25] Olivares-Marín M, Fernández-González C, Macías-García A, Gómez-Serrano V. Thermal behaviour of lignocellulosic material

in the presence of phosphoric acid: influence of the acid content in the initial solution. Carbon, **44**, 2347 (2006). http://dx.doi.org/10.1016/j.carbon.2006.04.004.

[26] Jibril B, Houache O, Al-Maamari R, Al-Rashidi B. Effects of H_3PO_4 and KOH in carbonization of lignocellulosic material. J Anal Appl Pyrolysis, **83**, 151 (2008). http://dx.doi.org/10.1016/j.jaap.2008.07.003.

[27] Jin X, Lee CH, Kim JH, You DJ, Pak C, Shon JK, Kim JM. Systematically controlled pore system of ordered mesoporous carbons using phosphoric acid as the in situ generated catalysts for carbonization and activation. Bull Korean Chem Soc, **36**, 2062 (2015). http://dx.doi.org/10.1002/bkcs.10399.